JACS Au
AN OPEN ACCESS JOURNAL OF THE AMERICAN CHEMICAL SOCIETY

pubs.acs.org/jacsau
Article

Electric Field-Assisted Agglomeration of Trace Nanoparticle Impurities for Ultrahigh Purity Chemicals

Dongryul Lee,[‖] Donggyu Lee,[‖] Sungjune Lee, Hee Jeong Park, Kuk Nam Han, Sam-Jong Choi, Yun Ho Kim,* and Jihyun Kim*

Cite This: *JACS Au* 2024, 4, 1031−1038
Read Online

ABSTRACT: With the advancement of semiconductor manufacturing technology, the effects of trace impurities in industrial chemicals have grown significantly. In industrial processes, conventional purification methods, such as filtration and distillation, have reached their limits for removing nanoparticles from aqueous and acidic solutions. Especially, silicon and silicate are two fundamental byproducts in semiconductor fabrication processes. Assembly and subsequent removal of these materials at the nanoparticle level have been confronted with significant challenges. Therefore, it is imperative to develop technologies to effectively control and remove these impurities for next-generation manufacturing processes. In this study, we explored the use of electric field-assisted assembly to agglomerate silicate and silicon nanoparticles in industry-standard aqueous and acidic solutions. By applying an alternating current electric field, we induced dipole moments in the nanoparticles, which led to their agglomeration. Notably, nanoparticles smaller than 4 nm grew into significantly larger ones, with submicroparticle sizes exceeding 87 nm for silicate and reaching 130 nm for silicon. Through systematic analysis of the size distribution changes, we identified optimal agglomeration times of 10 min for silicate and 20 min for silicon, revealing effective agglomeration within the frequency range of 1−1000 kHz. The agglomerated particles were stable for 5 days. Our electric field-assisted approach to obtain assembled nanoparticles that can be subsequently removed by conventional purification processes holds promise for enhancing future microfabrication processes, such as semiconductor manufacturing, potentially improving the manufacturing yield and uniformity by reducing the number of trace particles that can act as defective sites.

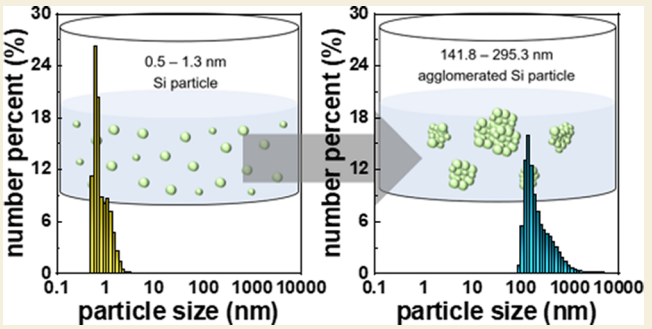

KEYWORDS: *electric field, agglomeration, nanoparticle, dielectrophoresis, polarization*

INTRODUCTION

Technological advancements have led to continuously advancing manufacturing processes, particularly in industries such as semiconductor production, which require small, powerful, and high-performance devices. As device miniaturization progresses to the submicrometer scale, manufacturing margins become narrower, making the effects of trace impurities in chemicals increasingly pronounced. Minute impurities or nanoparticles in chemicals can cause defects, significantly decreasing the device production yields. Conventional purification methods, such as filtration, distillation, and ion exchange, have been employed to mitigate impurities in chemicals at the micron scale. However, the removal efficacy of these methods has reached fundamental limits for microorganisms or nanoparticles. In addition, acidic solutions, including HF, HNO_3, and H_2SO_4, which are widely used to obtain highly clean surfaces, encounter limitations in achieving ultrahigh purity. Currently, the most widely used chemical purification systems are distillation and filtration. Although an increasing number of columns are required to remove trace impurities using distillation towers, their purification efficiency is very low. For commercially available filters, the pore size is insufficient to trap all subnanoparticles present in the material. Moreover, as the pore size of the filters decreased, the permeation flux also decreased, limiting the mass production of purified chemicals. It is essential to develop a technology that can control and aggregate nanoparticles for the effective removal of several nanometers. Therefore, alternative purification methods need to be explored to meet the specifications of next-generation manufacturing processes.

Research on the assembly and removal of nano- and submicron-sized particles using electric fields is well documented.[1−4] The assembly and movement of charged particles along the electric field facilitate their removal, whereas for

Received: December 2, 2023
Revised: January 8, 2024
Accepted: January 19, 2024
Published: February 6, 2024

https://doi.org/10.1021/jacsau.3c00765
JACS Au 2024, 4, 1031−1038

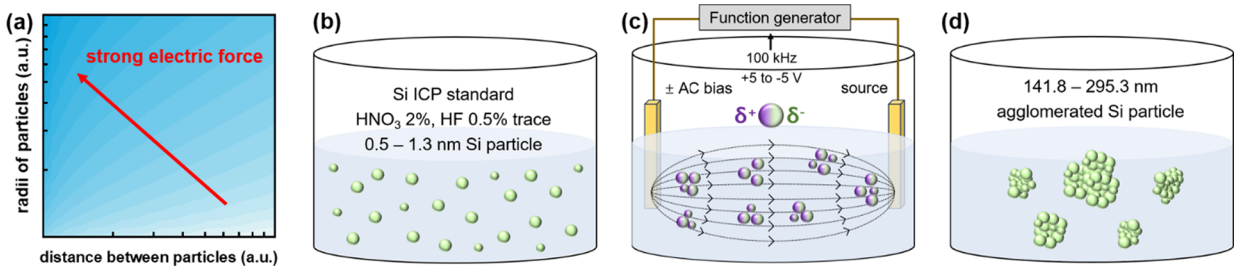

Figure 1. (a) Logarithmic representation of the electric force between two particles as a function of interparticle distance and particle radii, derived from eq 3. (b) Schematic of the DEP process of the ICP standard solution. Silicon and silicate ICP standard solutions were placed in a Teflon vial. (c) Function generator was connected to electrodes, and alternating current bias was applied. (d) Silicon and silicate nanoparticles agglomerated to larger particles.

neutral particles, induced dipoles facilitate assembly and removal.[5−8] Gao et al. used a direct current (DC) electric field to assemble a series of DNA networks on a large scale.[9] However, owing to their low energy consumption and outstanding performance, processes using pulsed and nonuniform electric fields for demulsification and dehydration have been reported.[10,11] Tsouris et al. enhanced the efficiency of distillation by applying an electric field.[12] Peng et al. reported that droplets in oil can coalesce under a high-voltage pulsed electric field.[13] Gong et al. modulated the size of particles with a pulsed-to-electric field by varying the electric field intensity and frequency.[14] Furthermore, neutral particles can be controlled in nonuniform electric fields by dielectrophoresis (DEP) force, facilitating the creation of particle clusters.[15,16] Opoku et al. achieved the alignment of ZnO nanowire powder, suitable for transistor channels, using DEP deposition.[17] Krupke et al. demonstrated the separation of metallic and semiconducting single-walled carbon nanotubes with different dielectric constants through DEP processes at varying frequencies.[18] Under alternating current (AC), polarizable microparticles can generate charge separation, surface accumulation, and electric field-induced dipoles and coagulate into larger particles.[19−21]

This study demonstrates the potential of utilizing electric fields to efficiently assemble trace chemical impurities into clustered impurities of larger sizes that can be readily removed through conventional purification processes. Silicate and silicon, prevalent byproducts in semiconductor manufacturing processes such as etching and deposition, are unequivocally classified as particles requiring assembly. We demonstrated that the application of an electric field induces dipole moments in silicon and silicate nanoparticles, enabling the aggregation of nanoparticles measuring only several nanometers into particles on a scale of hundreds of nanometers. Silicon particles are one of the primary impurities in liquid chemicals that are difficult to remove completely using current purification processes owing to their small size, the existence of other impurities in different forms (ions, oligomers, and particles), and their chemical stability. Consequently, the application of an electric field was designed to align with the sizes and systems used in contemporary semiconductor processes, and the same was achieved at low voltages. We analyzed the aggregated particle size distribution using a Zetasizer and confirmed the stability of the aggregates over time and in various environments, including aqueous and acidic solutions.

RESULTS AND DISCUSSION

Based on research conducted by Peng et al., particles polarized by an electric field in a solution experience an attractive force, leading to their aggregation.[13] Assuming that μ_1 and μ_2 are the dipole moments of two polarized particles, the electric field energy (W) between the two polarized particles can be described as follows.

$$W = \frac{\mu_1\mu_2}{4\pi\varepsilon_0\varepsilon_2 d^3}(3\cos\theta^2 - 1) \tag{1}$$

$$\mu_1 = 4\pi r_1^3\varepsilon_0\varepsilon_2 E\left(\frac{\varepsilon_1 - \varepsilon_2}{\varepsilon_1 + 2\varepsilon_2}\right),\ \mu_2 = 4\pi r_2^3\varepsilon_0\varepsilon_2 E\left(\frac{\varepsilon_1 - \varepsilon_2}{\varepsilon_1 + 2\varepsilon_2}\right) \tag{2}$$

where d is the distance between two particles, r_1 and r_2 are the radii of two particles, ε_0 is the vacuum dielectric constant, ε_1 and ε_2 are the relative dielectric constants of the particle and solution, respectively, and E is the intensity of the electric field. By partially differentiating the electric field energy with respect to d, the electric force between the two particles can be calculated as follows:

$$F_d = -\frac{\partial W}{\partial d} = -\frac{6\pi\varepsilon_0\varepsilon_2 r_1^3 r_2^3 E^2}{d^4} \times \left(\frac{\varepsilon_1 - \varepsilon_2}{\varepsilon_1 + 2\varepsilon_2}\right)^2 \times (3\cos 2\theta + 1) \tag{3}$$

From the above equation, it can be inferred that the primary factors influencing particle aggregation are the distance between the particles (d) and the radii of the particles (r_1 and r_2).

Figure 1a shows a logarithmic scale representation of the electric force between two particles, modeled as a function of their interparticle distance and respective radii, derived from eq 3. A reduced distance between particles coupled with an increase in particle size results in a stronger electric attractive force. As the electric field density gradient increases in a solution with silicon particles, the interparticle distance decreases due to the negative DEP (nDEP) phenomenon. As the interparticle distance decreased, the attractive force F_d between the silicon particles increased exponentially, providing a sufficient driving force for the silicon nanoparticles to aggregate and grow into larger particles.

When polarizable nanoparticles are exposed to a nonuniform electric field, they undergo movement owing to the DEP force based on the electric field density gradient. The DEP force is represented by the following equation:

$$F_{DEP} = A\varepsilon_m Re(F_{CM})\nabla|E^2| \tag{4}$$

where A is a value related to geometric shape and volume of the particle, $Re(F_{CM})$ is the real part of the Clausius−Mossotti

https://doi.org/10.1021/jacsau.3c00765
JACS Au 2024, 4, 1031−1038

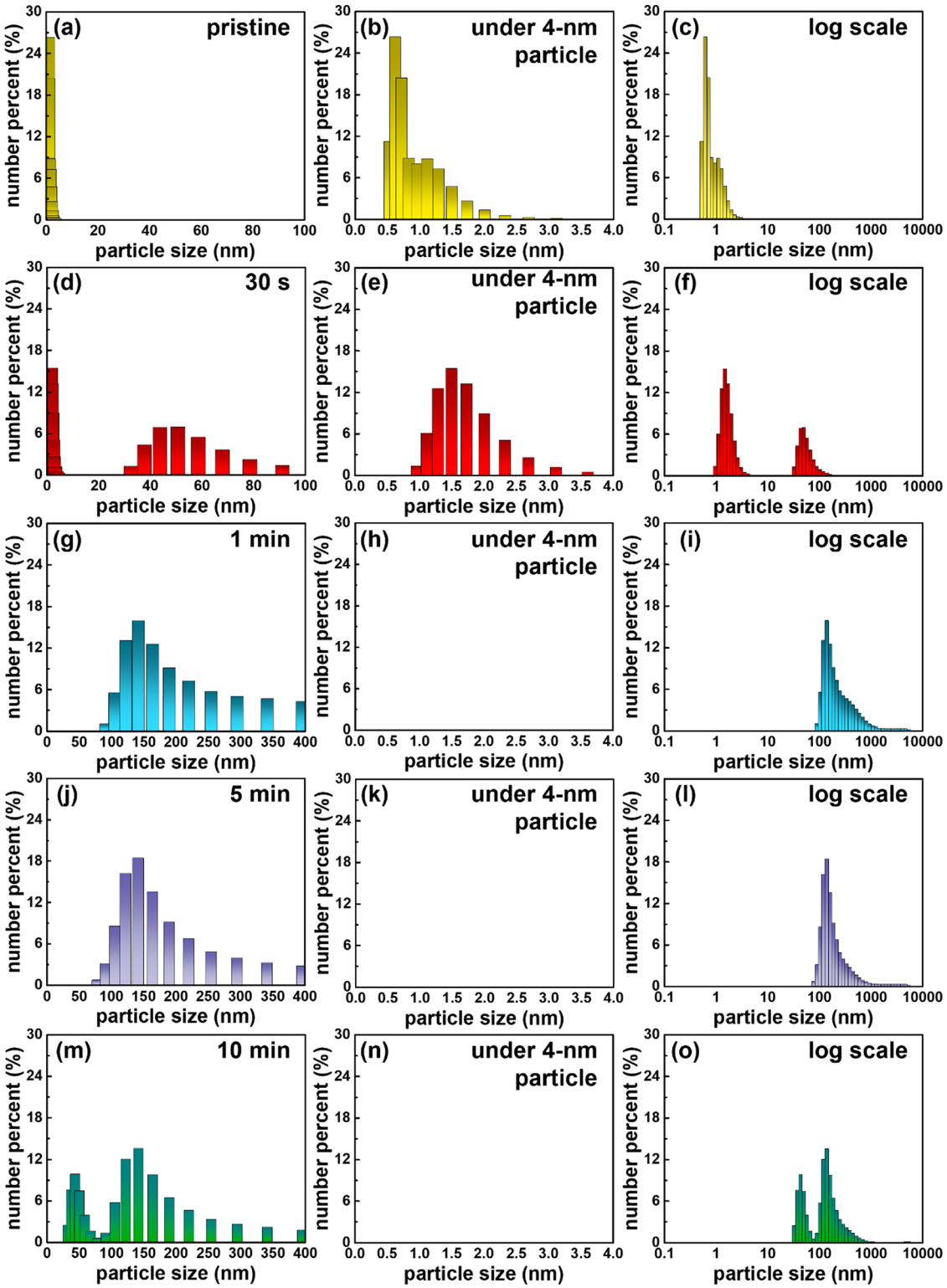

Figure 2. Atomic number percentage of silicate nanoparticle in the silicate ICP standard aqueous solution (a–c) before DEP process and after (d–f) 30 s, (g–i) 1 min, (j–l) 5 min, and (m–o) 10 min of DEP time with log scale graph.

factor, and $\nabla|E^2|$ is the gradient of the square of the electric field. The Clausius–Mossotti factor (F_{CM}), which determines the direction and magnitude of the DEP force based on the frequency change in the AC voltage, is defined as follows:

$$F_{CM} = \frac{\varepsilon_p^* - \varepsilon_m^*}{\varepsilon_m^*} \tag{5}$$

$$\varepsilon_p^* = \varepsilon_p - i\frac{\sigma_p}{\omega}, \quad \varepsilon_m^* = \varepsilon_m - i\frac{\sigma_m}{\omega} \tag{6}$$

where ε_p^* and ε_m^* are the complex permittivities of the particle and medium, respectively, i is $\sqrt{-1}$, and ω is the frequency of the electric field. ε_p and ε_m are the dielectric constants of the

https://doi.org/10.1021/jacsau.3c00765
JACS Au 2024, 4, 1031–1038

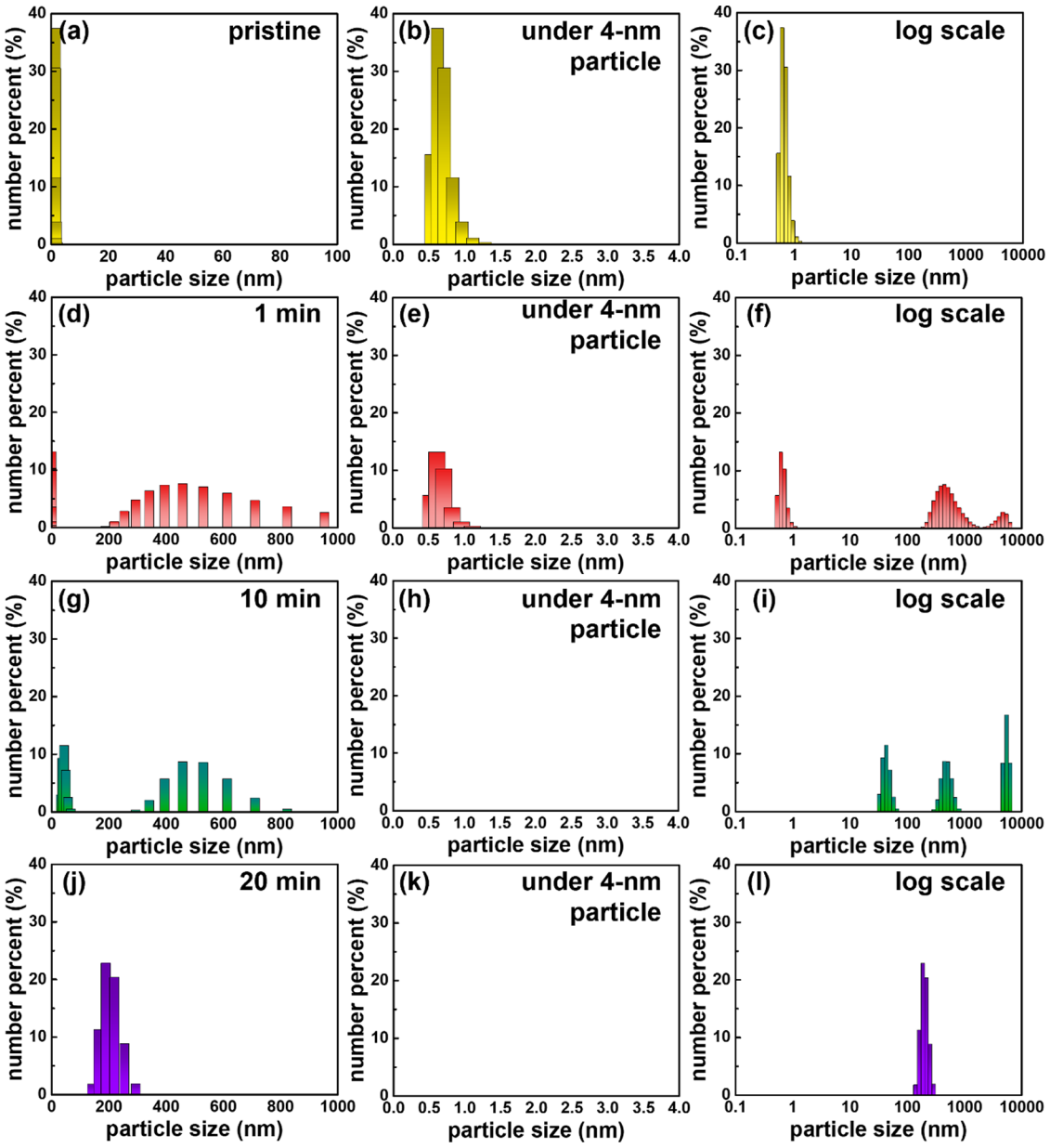

Figure 3. Atomic number percentage of silicon nanoparticle in the silicon ICP standard acid solution (a–c) before DEP process and after (d–f) 1 min, (g–i) 10 min, and (j–l) 20 min of DEP time with log scale graph.

particle and medium, respectively, and σ_p and σ_m are the conductivities of the particle and medium, respectively.

Figure 1b–d illustrates the electric field-assisted assembly and separation processes in a standard inductively coupled plasma (ICP) solution. The ICP standard solution contained only nanoparticles smaller than 4 nm at a concentration of 0.1%, making it suitable for nanoparticle agglomeration. Two types of ICP standard solutions were used: one with distributed silicon particles and the other with silicate particles. The silicon nanoparticles in the silicon ICP standard solution were dispersed in 2% HNO_3 and 0.5% HF acid solutions to prevent nanoparticle agglomeration. Conversely, the silicate nanoparticles in the silicate ICP standard solution were dispersed in an aqueous form. Nanoparticles ranged in diameter from 0.5 to 1.3 nm in both solutions with a concentration of 0.1%. A function generator was utilized to generate a sine-wave-shaped AC voltage with a frequency of 100 kHz at an amplitude of 10 peak-to-peak voltages (V_{pp}), which can be readily obtained from commercial equipment. A gold tip was connected to the function generator to form a circuit and maintain a consistent voltage application under acidic conditions. This voltage can induce the effective movement of the particles and a dipole moment within the individual particles, enabling particle agglomeration.

Figure S1 shows the real part of the Clausius–Mossotti factor of silicon as a function of the frequency. The Clausius–Mossotti factor facilitates the prediction of both the magnitude and direction of the DEP force exerted on the silicon nanoparticles at varying frequencies. The calculated results for the silicon ICP standard acid solution containing 2% HNO_3 and 0.5% HF showed that the DEP force acting on the silicon nanoparticles remained constant up to 10 GHz, and subsequently decreased at frequencies higher than 10 GHz. Silicon nanoparticles, owing to their lower dielectric constant, tend to migrate toward regions

https://doi.org/10.1021/jacsau.3c00765
JACS Au 2024, 4, 1031–1038

with lower electric field densities, a phenomenon known as nDEP. This behavior can be ascertained from the negative real component of the Clausius−Mossotti factor. Microparticles experience a greater DEP force than nanoparticles because the DEP force is proportional to the volume. However, controlling the nanoparticles with DEP has been confirmed in several studies. Brown et al. utilized an atomic force microscope tip at the nm scale to control the behavior of silicon nanoparticles with a radius of 5 nm in water.[22] Chinappi et al. proposed an analytical model that uses DEP to adjust the position of polarized nanoparticles within a nanopore.[23]

Figure 2 shows the Zetasizer analysis results of the silicate ICP standard solution (aqueous) before and after the electric field-assisted assembly over time. The silicate ICP standard solution was treated with an AC electric field for 0.5, 1, 5, 10, 30, and 60 min. The silicate ICP standard solution contained SiO_4^{4-} molecules linked in a few patterns, and the solution in its pristine state was analyzed to examine the distribution of silicate nanoparticles in the solution. Figure 2b,c shows that only silicate particles ranging from 0.5 to 3.6 nm are distributed in the pristine ICP solution, with particles of size 0.6 nm constituting the highest proportion. Because the Si−O bond of the silicate molecule has a dipole moment of 4.1803, it can produce a sufficient amount of charge separation and accumulation even with a short duration of voltage application. The distance between the two electrodes was maintained at 2 in to ensure that the processing conditions were compatible with industry-standard cleaning processes. Previous research efforts have narrowed the distance between the electrodes to tens to hundreds of micrometers to reduce the required voltage. However, the objective of this study was not electrode alignment, but rather to induce agglomeration in the solution through the application of an electric field. Therefore, a large-scale environment suitable for commercial industrial applications was established.

As shown in Figure 2, the electric field-assisted assembly process is conducted at a frequency of 100 kHz and a sine-wave-shaped AC voltage with an amplitude of 10 V_{pp}. The measurements show that 4 nm undersized particles agglomerate to form medium-sized particles in the range of 30−100 nm after 30 s (Figure 2f). The duration was varied to analyze the effect of the electric field application time on the size distribution of the particles. After 1 min of treatment, all nanoparticles smaller than 4 nm agglomerated in the range of 87−1460 nm, with a peak distribution at 141 nm (Figure 2i). Extending the electric field treatment time to 5 min yielded similar results (Figure 2j−l). At 10 min, some of the agglomerated medium-sized particles separated again, resulting in relatively smaller particles in the range of 31−80 nm (Figure 2o). However, at 30 and 60 min, the particles clustered to form particles larger than 87 nm (Figure S2). During the electric field-assisted assembly treatment, medium-sized particles agglomerate as long as minimum agglomeration time is achieved. With additional treatment time, some particles broke down and reagglomerated. Therefore, nanoparticles smaller than 4 nm in the silicate ICP standard solution can agglomerate into medium-sized particles larger than 87 nm. The size of these agglomerated particles varies according to the dipole moment, which is influenced by the properties of the silicate particles, and the particle size distribution changes depending on the treatment time. This finding enabled the purification of nanoparticles by using a conventional filtration process with a 10 nm pore size filter. Furthermore, we conducted energy-dispersive X-ray spectroscopy (EDX) analysis to confirm that the particles aggregated by the applied electric field are silica (Figure S3). When the LUDOX solution, which has a higher weight% of silica than the silicate ICP standard solution, was treated at a frequency of 100 kHz for 15 min, a substance expected to be silica was discovered on the metal electrode. After the elements of this particle were analyzed using EDX, the atomic percentages of Si and O were found to be 9.51 and 65.27, respectively (Table S1). The atomic percentages of Si and O in the agglomerated particles proved that they were agglomerated silica.

Figure 3 shows the Zetasizer analysis results before and after time-dependent electric field treatment of the silicon ICP standard (2% HNO_3 and 0.5% HF acid solutions). The silicon ICP standard solution was treated with an AC electric field for 1, 10, and 20 min. Intrinsically, the silicon ICP solution includes Si atoms that are semiconjugated, and to preclude spontaneous agglomeration within the ICP solution, it is maintained in a weak HF trace condition. Examination of the particle distribution in the pristine solution revealed the exclusive presence of silicon nanoparticles ranging from 0.5 to 1.3 nm, with the 0.6 nm particle being the most predominant (Figure 3b,c). Given the absence of covalent bonds between the silicon particles in solution, there was no associated dipole moment. Therefore, the application of a nonuniform electric field induces the partial agglomeration of some silicon particles. A processing duration longer than that of silicate was used to ensure sufficient agglomeration at the same frequency as that of the silicate electric field-assisted assembly treatment to predict the electrical imbalance within the agglomerating particles.

After 1 min of treatment, more than 60% of the particles less than 4 nm in size agglomerated into medium-sized particles 100 nm or larger. However, nanoparticles smaller than 4 nm remained, and the size of the agglomerated particles exhibited some variation (Figure 3d−f). After 10 min of treatment, the scattered distribution of medium-sized particles was concentrated between 400 and 600 nm, and nanoparticles smaller than 4 nm were fully agglomerated (Figure 3g,h). There were slight variations among the medium-sized particles in the range of 30−100 nm, the large particles in the range of 330−807 nm, and the superlarge particles in the range of 4400−7200 nm. This phenomenon is attributed to the fact that during the electric field-assisted assembly, some particles arbitrarily form larger clusters, and owing to subsequent fragmentation, do not achieve a fully stable state (Figure 3i). Following a 20-min treatment, nanoparticles less than 4 nm are no longer present, and they all agglomerated into medium-sized particles in the range 130−330 nm (Figure 3j−l). Therefore, nanoparticles smaller than 4 nm in size within the silicon ICP standard solution can agglomerate into medium- to large-sized particles of 130 nm or larger through this electric field process. Similar to silicates, the size of the particles is determined by the formation of the particle dipole moment owing to the electric field process, and as the processing time increases, the particle size distribution narrows. Consequently, the purification of nanoparticles can be achieved using a filtration process with a conventional filter. Traditional acidic solution purification methods, such as distillation, have limitations in terms of process complexity, danger, and productivity. However, purification of acidic solutions through electric field-assisted assembly treatment, as described above, offers advantages, such as simplicity, safety, and fast processing speed.

In general, the agglomeration, separation, and coalescence of droplets and nano/microparticles are achieved by using an AC

https://doi.org/10.1021/jacsau.3c00765
JACS Au 2024, 4, 1031−1038

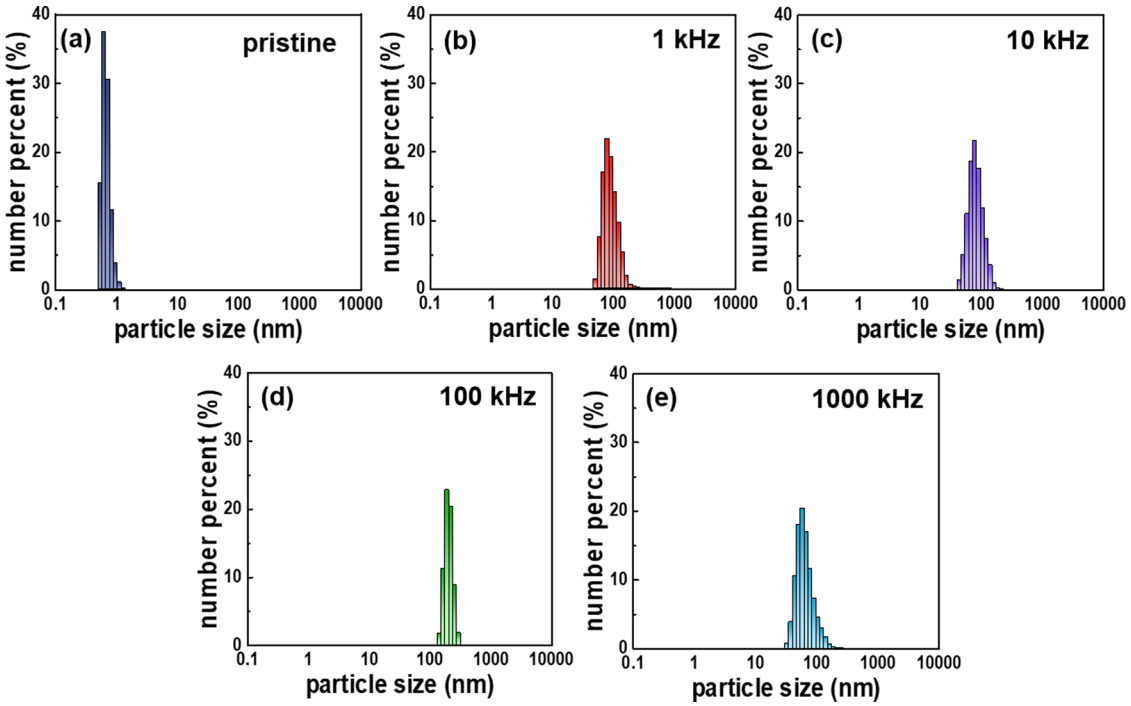

Figure 4. Atomic number percentage of silicon nanoparticle in (a) pristine solution and after 20 min of DEP process at varying frequencies (b) 1, (c) 10, (d) 100, and (e) 1000 kHz.

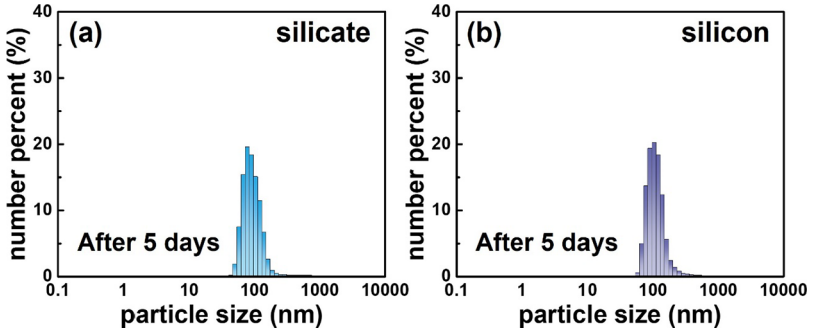

Figure 5. Atomic number percentage of (a) silicon and (b) silicate nanoparticles in the solution 5 days after completion of the DEP process.

bias or pulsed bias rather than a DC bias. External electric fields induce dipole moments in particles within the fluid in different directions. By continuously changing the direction of the nonuniform electric field, AC or pulsed bias can correct the optimal dipole position within the particles and enhance the strength of the induced dipole. Although colloids or nanoparticles present in the fluid are randomly distributed in various directions through AC bias, the random distribution of these particles can be electrokinetically aligned to induce an effective dipole and trigger movement and coagulation. Furthermore, the nonuniform AC bias enhances the strength of an individual dipole and strengthens the induced dipole in agglomerated particles, facilitating their coalescence into medium- or large-sized particles. Kim et al. reported that using AC DEP provides better alignment with a higher yield rate than using DC DEP.[24] Based on the advantages of an AC electric field, efficient movement control and assembly of silicate and silicon particles can be achieved. The agglomeration characteristics of the nanoparticles in the silicon ICP standard acid solution are analyzed at frequencies of 1, 10, 100, and 1000 kHz and 20 min of treatment to determine the stable frequency operating range (Figure 4a–e). Figure 4a confirms that only silicon particles smaller than 4 nm exist in the pristine silicon ICP standard solution. Subsequent processes at each frequency showed that the size and proportion of the agglomerated particles varied slightly; however, all of the particles agglomerated into medium-sized particles larger than 50 nm. For 1 and 10 kHz, particles of 78.8 nm constituted the highest proportion, and the agglomerated particles based on these particles exhibited standard deviations of 32.3 and 24.2 nm, respectively. At 100 kHz, particles measuring 190.1 nm were predominant, with a standard deviation of 36.11. At 1000 kHz, particles measuring 58.8 nm were predominant, with a standard deviation of 24.1. The standard deviations suggest that the primary dispersion range was ±24–36 nm based on the particles with the highest percentage across all frequencies. Therefore, a frequency range consistent with the theoretical Clausius–Mossotti factor calculation results was effectively applied to the actual process. Based on the standard deviation results, it was anticipated that using a filter with a pore size of 100 nm and a frequency of 100 kHz would enable the filtration of agglomerated particles. Filters with pore sizes of less than 30 nm were estimated to be capable of filtering agglomerated particles. To examine the stable operating frequency range, the real part of the Clausius–

https://doi.org/10.1021/jacsau.3c00765
JACS Au 2024, 4, 1031–1038

Mossotti factor is calculated as a function of the frequency. The calculated results for the silicate ICP standard solution showed that the DEP force acting on the silicate nanoparticles remained constant up to 1 MHz, and subsequently decreased at frequencies higher than 10 MHz (Figure S4a). The agglomeration characteristics of the nanoparticles in the silicate ICP standard solution are further analyzed at frequencies of 1, 10, 100, and 1000 kHz for a 10-min treatment (Figure S4b–f). The silicate nanoparticles in the silicate ICP standard solution showed a stable operating performance within this range, which was consistent with the theoretical Clausius–Mossotti factor calculation.

Zetasizer measurements are conducted on a solution stored for 5 days after the process to determine whether the agglomerated particles maintained the same level of agglomeration over time (Figure 5). Silicate and silicon nanoparticles exhibited sustained agglomeration with sizes ranging from 50.8 to 712.4 nm, even after 5 days. In particular, silicon nanoparticles exist in pristine ICP standard solutions in a HF trace atmosphere, preventing agglomeration over time in the solution. Although HF was present in the solution after the electric field treatment in the same manner as reported previously, it did not disaggregate the agglomerated particles. Therefore, the particles that agglomerated after the electric field-assisted assembly process maintained a stable agglomerated state, unless they were subjected to external pressure. This finding indicates that the agglomeration effect induced by the electric field was not temporary. The stability of these agglomerated silicate and silicon particles suggests that the particle agglomeration effect was not compromised in the subsequent purification processes, making effective filtration highly desirable.

EXPERIMENTAL METHODS

Electro-Field-Driven Assembly Process

Silicate (Silicate Standard for IC, Sigma-Aldrich), silicon standard solutions (Silicon Standard for ICP, Sigma-Aldrich), and colloidal silica (LUDOX SM colloidal silica, Sigma-Aldrich) were used. The gold electrodes were cleaned meticulously with acetone, isopropyl alcohol, and ethanol for several minutes. The cleaned electrodes were then placed in Teflon vials containing the standard silicate and silicon solutions. A pair of gold electrodes was connected to an Agilent 33250A 80 MHz function/arbitrary waveform generator. An AC of 10 V_{PP} was applied at a frequency of 100 kHz under various time conditions. After the electric field-assisted assembly process, the treated solution was transferred to another Teflon vial.

Analysis

The solution was analyzed using a Zetasizer (Nano ZS, Malvern Panalytical) to characterize the particle size and distribution. Scanning transmission electron microscopy (GeminiSEM 560, ZEISS) was used to examine the agglomerated silica particle morphology. EDX was used to investigate the elemental composition of the agglomerated silica particles which are mounted on carbon tape.

CONCLUSIONS

Our study demonstrated the feasibility of electric field-assisted agglomeration of silicates and silicon nanoparticles. We elucidated that the application of an AC electric field induces a dipole moment, which causes agglomeration. Notably, when the nanoparticles are smaller than 4 nm, they grow into significantly larger particles, with silicate and silicon particles reaching 87 and 130 nm, respectively. By analysis of the particle size distribution, the optimal agglomeration times were identified to be 10 and 20 min for silicate and silicon, respectively. The Clausius–Mossotti factor indicated effective agglomeration between 1 and 1000 kHz, which was confirmed by the experimental results at varying frequencies. The agglomerated particles remained stable for more than 5 days. The electric field-assisted agglomeration of nanoparticles is expected to enhance the yield of future semiconductor microfabrication processes, offering a promising avenue for advancing semiconductor manufacturing.

ASSOCIATED CONTENT

Supporting Information

The Supporting Information is available free of charge at https://pubs.acs.org/doi/10.1021/jacsau.3c00765.

Clausius–Mossotti plot, atomic number percentage of nanoparticles, and SEM data (PDF)

AUTHOR INFORMATION

Corresponding Authors

Yun Ho Kim − *Material Technology Team, Samsung Electronics, Hwaseong-si, Gyeonggi-do 18448, South Korea*; Email: yunho17.kim@samsung.com

Jihyun Kim − *Department of Chemical and Biological Engineering, Seoul National University, Seoul 08826, South Korea*; orcid.org/0000-0002-5634-8394; Email: jihyunkim@snu.ac.kr

Authors

Dongryul Lee − *Department of Chemical and Biological Engineering, Korea University, Seoul 02841, South Korea*

Donggyu Lee − *Department of Chemical and Biological Engineering, Seoul National University, Seoul 08826, South Korea*

Sungjune Lee − *Material Technology Team, Samsung Electronics, Hwaseong-si, Gyeonggi-do 18448, South Korea*

Hee Jeong Park − *Material Technology Team, Samsung Electronics, Hwaseong-si, Gyeonggi-do 18448, South Korea*

Kuk Nam Han − *Material Technology Team, Samsung Electronics, Hwaseong-si, Gyeonggi-do 18448, South Korea*

Sam-Jong Choi − *Material Technology Team, Samsung Electronics, Hwaseong-si, Gyeonggi-do 18448, South Korea*

Complete contact information is available at: https://pubs.acs.org/10.1021/jacsau.3c00765

Author Contributions

[‖]D.L. and D.L. contributed equally to this work. CRediT: **Sungjune Lee** investigation, methodology, validation, writing-review & editing; **Hee Jeong Park** investigation, methodology, supervision, writing-review & editing; **Kuk Nam Han** investigation, methodology, validation, writing-review & editing; **Sam-Jong Choi** project administration, supervision; **Yun Ho Kim** project administration, supervision, writing-review & editing.

Notes

The authors declare no competing financial interest.

ACKNOWLEDGMENTS

This work was supported by Samsung Electronics Co., Ltd (IO220907-02384-01) and Korea Institute for Advancement of Technology (KIAT) grant funded by the Korea Government

(P0012451, The Competency Development Program for Industry Specialist).

REFERENCES

(1) Liu, M.; Yang, M.; Wan, X.; Tang, Z.; Jiang, L.; Wang, S. From Nanoscopic to Macroscopic Materials by Stimuli-Responsive Nanoparticle Aggregation. *Adv. Mater.* **2023**, *35* (20), No. e2208995.
(2) Li, S.; He, J.; Xu, Q.-H. Aggregation of Metal-Nanoparticle-Induced Fluorescence Enhancement and Its Application in Sensing. *ACS Omega* **2020**, *5* (1), 41−48.
(3) Pereira, R. N.; Souza, B. W. S.; Cerqueira, M. A.; Teixeira, J. A.; Vicente, A. N. A. Effects of Electric Fields on Protein Unfolding and Aggregation: Influence on Edible Films Formation. *Biomacromolecules* **2010**, *11* (11), 2912−2918.
(4) Karpov, S. V.; Gerasimov, V. S.; Isaev, I. L.; Markel, V. A. Local Anisotropy and Giant Enhancement of Local Electromagnetic Fields in Fractal Aggregates of Metal Nanoparticles. *Phys. Rev. B* **2005**, *72* (20), No. 205425.
(5) Pethig, R. Dielectrophoresis: Status of the Theory, Technology, and Applications. *Biomicrofluidics* **2010**, *4* (2), No. 022811.
(6) Gascoyne, P. R. C.; Vykoukal, J. Particle Separation by Dielectrophoresis. *Electrophoresis* **2002**, *23* (13), 1973−1983.
(7) Lapizco-Encinas, B. H.; Rito-Palomares, M. Dielectrophoresis for the Manipulation of Nanobioparticles. *Electrophoresis* **2007**, *28* (24), 4521−4538.
(8) Dellarosa, N.; Ragni, L.; Laghi, L.; Tylewicz, U.; Rocculi, P.; Dalla Rosa, M. Time Domain Nuclear Magnetic Resonance to Monitor Mass Transfer Mechanisms in Apple Tissue Promoted by Osmotic Dehydration Combined with Pulsed Electric Fields. *Innov. Food Sci. Emerg. Technol.* **2016**, *37*, 345−351.
(9) Gao, M.; Hu, J.; Wang, Y.; Liu, M.; Wang, J.; Song, Z.; Xu, H.; Hu, C.; Wang, Z. Controlled Self-Assembly of λ-DNA Networks with the Synergistic Effect of a DC Electric Field. *J. Phys. Chem. B* **2019**, *123* (46), 9809−9818.
(10) Semenoglou, I.; Dimopoulos, G.; Tsironi, T.; Taoukis, P. Mathematical Modelling of the Effect of Solution Concentration and the Combined Application of Pulsed Electric Fields on Mass Transfer During Osmotic Dehydration of Sea Bass Fillets. *Food and Bioprod. Process.* **2020**, *121*, 186−192.
(11) Traffano-Schiffo, M. V.; Laghi, L.; Castro-Giraldez, M.; Tylewicz, U.; Romani, S.; Ragni, L.; Dalla Rosa, M.; Fito, P. J. Osmotic Dehydration of Organic Kiwifruit Pre-Rreated by Pulsed Electric Fields: Internal Transport and Transformations Analyzed by NMR. *Innov. Food Sci. Emerg. Technol.* **2017**, *41*, 259−266.
(12) Tsouris, C.; Blankenship, K. D.; Dong, J.; DePaoli, D. W. Enhancement of distillation efficiency by application of an electric field. *Ind. Eng. Chem. Res.* **2001**, *40* (17), 3843−3847.
(13) Peng, Y.; Liu, T.; Gong, H.; Zhang, X. Review of the Dynamics of Coalescence and Demulsification by High-Voltage Pulsed Electric Fields. *Int. J. Chem. Eng.* **2016**, *2016*, 1−8.
(14) Gong, H.; Yu, B.; Peng, Y.; Dai, F. Promoting Coalescence of Droplets in Oil Subjected to Pulsed Electric Fields: Changing and Matching Optimal Electric Field Intensity and Frequency for Demulsification. *J. Dispers. Sci. Technol.* **2019**, *40* (9), 1236−1245.
(15) Constantinou, M.; Rigas, G. P.; Castro, F. A.; Stolojan, V.; Hoettges, K. F.; Hughes, M. P.; Adkins, E.; Korgel, B. A.; Shkunov, M. Simultaneous Tunable Selection and Self-Assembly of Si Nanowires from Heterogeneous Feedstock. *ACS Nano* **2016**, *10* (4), 4384−4394.
(16) Kolosnjaj-Tabi, J.; Gibot, L.; Fourquaux, I.; Golzio, M.; Rols, M.-P. Electric Field-Responsive Nanoparticles and Electric Fields: Physical, Chemical, Biological Mechanisms and Therapeutic Prospects. *Adv. Drug Delivery Rev.* **2019**, *138*, 56−67.
(17) Opoku, C.; Hoettges, K. F.; Hughes, M. P.; Stolojan, V.; Silva, S. R. P.; Shkunov, M. Solution Processable Multi-Channel ZnO Nanowire Field-Effect Transistors with Organic Gate Dielectric. *Nanotechnology* **2013**, *24* (40), No. 405203.
(18) Krupke, R.; Hennrich, F.; Löhneysen, H. V.; Kappes, M. M. Separation of Metallic from Semiconducting Single-Walled Carbon Nanotubes. *Science* **2003**, *301* (5631), 344−347.
(19) Rajnak, M.; Kurimsky, J.; Dolnik, B.; Kopcansky, P.; Tomasovicova, N.; Taculescu-Moaca, E. A.; Timko, M. Dielectric-Spectroscopy Approach to Ferrofluid Nanoparticle Clustering Induced by an External Electric Field. *Phys. Rev. E* **2014**, *90* (3), No. 032310.
(20) Evans, D. R.; Basun, S. A.; Cook, G.; Pinkevych, I. P.; Reshetnyak, V. Y. Electric Field Interactions and Aggregation Dynamics of Ferroelectric Nanoparticles in Isotropic Fluid Suspensions. *Phys. Rev. B* **2011**, *84* (17), No. 174111.
(21) Grzelczak, M.; Liz-Marzán, L. M.; Klajn, R. Stimuli-Responsive Self-Assembly of Nanoparticles. *Chem. Soc. Rev.* **2019**, *48* (5), 1342−1361.
(22) Brown, K. A.; Westervelt, R. M. Proposed Triaxial Atomic Force Microscope Contact-Free Tweezers for Nanoassembly. *Nanotechnology* **2009**, *20* (38), No. 385302.
(23) Chinappi, M.; Yamaji, M.; Kawano, R.; Cecconi, F. Analytical Model for Particle Capture in Nanopores Elucidates Competition among Electrophoresis, Electroosmosis, and Dielectrophoresis. *ACS Nano* **2020**, *14* (11), 15816−15828.
(24) Kim, T. H.; Lee, S. Y.; Cho, N. K.; Seong, H. K.; Choi, H. J.; Jung, S. W.; Lee, S. K. Dielectrophoretic Alignment of Gallium Nitride Nanowires (GaN NWs) for Use in Device Applications. *Nanotechnology* **2006**, *17* (14), 3394−3399.

https://doi.org/10.1021/jacsau.3c00765
JACS Au 2024, 4, 1031−1038